Synchronization Dynamics in Dementia: A Kuramoto Model Analysis of EEG Activity in Alzheimer's Disease and Frontotemporal Dementia

Ryan George*

Abstract

Alzheimer's disease (AD) and frontotemporal dementia (FTD) are major neurodegenerative disorders that produce overlapping clinical symptoms but affect partially distinct neural systems. I investigate whether resting-state electroencephalography (EEG) synchronization dynamics can help distinguish AD, FTD, and cognitively normal healthy controls (CN). Using a publicly available clinical EEG dataset of 88 subjects, EEG activity was analyzed across five canonical frequency bands: Delta, Theta, Alpha, Beta, and Gamma. Each scalp electrode was modeled as an oscillator in a Kuramoto synchronization framework, allowing both global phase synchronization and pairwise electrode coupling to be quantified. Spectral band power, Kuramoto order parameters, electrode coupling matrices, and machine-learning classification were used to identify group-level differences. AD patients showed elevated band power across all frequency bands, consistent with diffuse cortical slowing and abnormal neural excitability, while FTD patients showed the lowest power across bands, suggesting more focal neural disruption. Kuramoto analysis revealed that healthy controls had stronger synchronization in slower bands, whereas both AD and FTD showed abnormal hyper-synchronization in faster Alpha and Beta bands. Electrode-coupling analysis further showed a shift from frontal-dominated connectivity in healthy controls to posterior-dominated coupling in disease groups. Machine-learning models classified AD, FTD, and CN subjects above chance, with a tuned support vector machine achieving the highest balanced accuracy of 55.6%. These findings suggest that Kuramoto-based EEG synchronization features capture meaningful differences in neurodegenerative brain dynamics and may provide useful biomarkers for distinguishing dementia subtypes.

GitHub: https://github.com/ryangeorgekj/Synchronization-Dynamics-in-Dementia

Introduction

Alzheimer's disease (AD) has reached critical proportions in 2026. In the United States alone, approximately 7.4 million Americans aged 65 and older currently live with clinical Alzheimer's dementia [2]. Globally, dementia affects about 57 million people and remains one of the leading causes of death and disability among older adults [12]. Financially, the burden is immense: health and long-term care costs for Alzheimer's disease and related dementias in the United States are projected to reach hundreds of billions of dollars per year, while the worldwide cost of dementia has been estimated at more than US $ 1.3 trillion [2, 12]. Because dementia is increasing with population aging, better tools are needed for early detection and for distinguishing between different forms of neurodegenerative disease.

Alzheimer's disease is the most common cause of dementia, but it is not the only major dementia syndrome. Frontotemporal dementia (FTD) is a group of neurodegenerative disorders caused by progressive degeneration of the frontal and temporal lobes [4]. Whereas AD often begins with episodic memory impairment, FTD more commonly presents with changes in personality,

*Castro Valley High School

social behavior, executive function, or language. [11, 4]. These symptoms can overlap with AD or psychiatric illness, making differential diagnosis difficult, especially in the early stages. Therefore, biomarkers that reflect regional brain activity and functional connectivity may help separate AD, FTD, and cognitively normal controls.

A critical area of AD research focuses on mitochondria-associated endoplasmic-reticulum membranes (MAMs), which are physical contact points between the endoplasmic reticulum and mitochondria [3]. The MAM hypothesis suggests that memory-related breakdown may begin with altered communication between these two organelles. In AD patients, MAM function can become dysregulated, disrupting cellular energy balance, calcium signaling, and cholesterol processing before the widespread appearance of amyloid plaques and neurofibrillary tangles [3].

Genetics also play a major role in AD risk. Genes such as *APOE*, expressed in support cells such as astrocytes, and *TREM2*, expressed in immune cells such as microglia, are associated with increased AD risk [6]. Down syndrome provides another important genetic connection to AD. Individuals with Down syndrome have three copies of chromosome 21, which contains the gene encoding amyloid precursor protein. This leads to lifelong overproduction of amyloid-related proteins, and most individuals with Down syndrome develop AD neuropathology by middle age, with many later developing dementia [7].

Patients with Alzheimer's disease contain two main types of pathological damage: amyloid plaques outside neurons and neurofibrillary tangles inside neurons [6]. Amyloid plaques form outside cells and can interfere with communication between neurons. These deposits can also build up on the walls of brain arterioles, weakening vessels and increasing vascular risk. While amyloid may act as an early trigger, tau pathology is closely associated with neuronal injury. In healthy neurons, tau is a microtubule-associated protein that stabilizes the internal transport tracks of the cell. In AD, tau becomes hyperphosphorylated and aggregates into tangles inside neurons, causing the internal structure of the neuron to collapse and eventually contributing to cell death [6]. As neurons die, the brain undergoes progressive atrophy. The fluid-filled cavities of the brain, called ventricles, expand as surrounding brain tissue shrinks. Ventricular enlargement can therefore serve as an imaging biomarker of AD progression, and MRI-based measures have been used to predict whether patients with mild cognitive impairment will progress to AD [10].

FTD has a different but partially overlapping biological profile. Instead of being defined primarily by amyloid plaques, FTD is commonly associated with abnormal accumulations of tau, TDP-43, or FUS proteins [4]. The affected brain regions are often concentrated in frontal and anterior temporal networks, which helps explain why FTD may cause early changes in inhibition, decision-making, empathy, language, and social behavior. Because AD and FTD damage different neural systems, they may also produce different patterns of electrical activity across scalp EEG electrodes.

Electroencephalography (EEG) is a useful tool for studying these diseases because it is non-invasive, relatively inexpensive, and measures brain activity with millisecond-level temporal resolution. Resting-state EEG studies of AD have often reported changes in spectral power and synchronization, including slowing of brain rhythms and altered functional connectivity [5]. More recent EEG datasets and machine-learning studies have made it possible to compare AD, FTD, and healthy controls directly using quantitative features from multiple frequency bands [8, 1]. In this study, EEG signals from AD, FTD, and cognitively normal subjects are analyzed using band power, Kuramoto synchronization, electrode-coupling matrices, and machine-learning classification. This approach tests whether abnormal synchronization dynamics can provide useful biomarkers for distinguishing dementia subtypes.

Methods

This work used the publicly available OpenNeuro dataset ds004504[9, 8]. The dataset contains resting-state, eyes-closed EEG recordings from 88 subjects: 36 patients with Alzheimer's disease (AD), 23 patients with frontotemporal dementia (FTD), and 29 cognitively normal healthy controls (CN). EEG activity was recorded from 19 scalp electrodes placed according to the international

10–20 system, covering frontal, temporal, central, parietal, and occipital brain regions.

The goal of the analysis was to determine whether EEG power and synchronization patterns could distinguish AD, FTD, and CN subjects. This is clinically relevant because AD and FTD can produce overlapping symptoms, but they often affect different neural systems. AD is commonly associated with diffuse cortical slowing and widespread network disruption, while FTD is more strongly associated with degeneration of frontal and temporal networks [4, 5].

EEG Preprocessing and Band Power

For each subject, EEG signals were separated into five standard frequency bands: Delta, Theta, Alpha, Beta, and Gamma. Bandpass filtering was applied separately for each band. After filtering, band power was computed for each electrode and frequency band, then averaged across electrodes to obtain one mean power value per subject per band.

Band power was used to measure how strongly each frequency range was represented in the EEG signal. This is important because neurodegenerative diseases often alter the balance between slow and fast brain rhythms. In AD, increased slow-wave activity is commonly interpreted as a marker of cortical dysfunction, while FTD may show more regionally specific changes.

Kuramoto Synchronization Analysis

The Kuramoto model was used to measure synchronization between EEG electrodes. In this framework, each electrode was treated as an oscillator whose phase changes over time. The Kuramoto phase equation is

$$\frac{d\theta_i}{dt} = \omega_i + \frac{K}{N}\sum_{j=1}^{N}\sin(\theta_j - \theta_i), \tag{1}$$

where θ_i is the phase of electrode i, ω_i is its natural frequency, K is the coupling strength, and N is the number of electrodes. The term $\sin(\theta_j - \theta_i)$ measures how much the phase of electrode j influences electrode i.

For each frequency band, the instantaneous phase of every electrode was extracted using the Hilbert transform. The overall level of synchronization across all 19 electrodes was then measured using the Kuramoto order parameter:

$$R(t) = \left| \frac{1}{N}\sum_{j=1}^{N} e^{i\theta_j(t)} \right|. \tag{2}$$

The value of $R(t)$ ranges from 0 to 1. A value close to 0 indicates weak synchronization across electrodes, while a value close to 1 indicates strong synchronization. For each subject and frequency band, the order parameter was averaged over time to obtain a single synchronization score.

In addition to global synchronization, pairwise coupling was computed between every pair of electrodes. This produced a 19×19 coupling matrix for each subject and frequency band. Each matrix represented how consistently two electrodes maintained a stable phase relationship over time.

Group-level coupling matrices were computed by averaging subject-level matrices within the AD, FTD, and CN groups. Disease-control difference matrices were then calculated by subtracting the CN coupling matrix from the AD and FTD matrices. Positive values indicated stronger coupling than healthy controls, while negative values indicated weaker coupling. These matrices were used to identify disease-related changes in functional connectivity across frequency bands.

Machine Learning Classification

Machine learning models were trained to classify subjects into AD, FTD, or CN groups using EEG-derived features. The feature set included band power, Kuramoto synchronization values, and electrode-coupling measurements across the five frequency bands.

Four supervised models were tested: Support Vector Machine (SVM), Random Forest, Logistic Regression, and a shallow Neural Network. Classification performance was evaluated using 5-fold cross-validation. Because there were three diagnostic groups, chance-level accuracy was approximately 33%. Balanced accuracy was used as the main performance metric because it accounts for differences in group size.

Random Forest feature importance was used to estimate which electrodes contributed most strongly to classification. Feature-importance values were grouped by electrode and averaged across frequency bands. This produced one importance score for each electrode.

The electrode-importance scores were visualized using both a bar chart and a scalp topomap. Electrodes with higher importance scores were interpreted as carrying more diagnostic information for distinguishing AD, FTD, and CN subjects.

Results

Band Power

Figure 1 illustrates the mean band power across all five frequency bands for each group. Alzheimer's Disease (AD) patients exhibited the highest band power across every frequency band, with the largest difference observed in the Delta band where AD showed 5.88×10^{-10} V^2/Hz compared to 3.27×10^{-10} V^2/Hz for Healthy Controls (CN) and 3.54×10^{-10} V^2/Hz for FTD. This pattern of elevated power across all bands in AD is consistent with known EEG biomarkers of diffuse cortical slowing and neural hyperexcitability. FTD patients consistently showed the lowest band power across all bands, suggesting more focal rather than diffuse neural changes compared to AD.

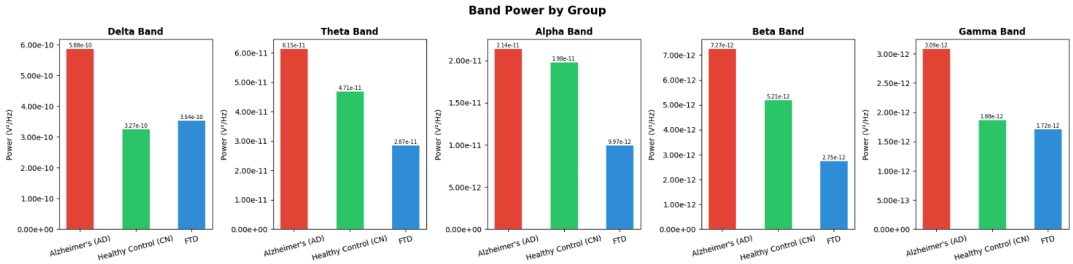

Figure 1: Mean band power (V^2/Hz) across five frequency bands — Delta, Theta, Alpha, Beta, and Gamma — for Alzheimer's Disease (AD), Healthy Controls (CN), and Frontotemporal Dementia (FTD). AD patients show consistently elevated power across all bands, while FTD patients show the lowest power throughout.

Kuramoto Synchronization

Figure 2 shows the Kuramoto order parameter across all five frequency bands. A striking reversal pattern was observed — Healthy Controls exhibited the highest synchronization in slower bands, with Delta CN = 0.949 and Theta CN = 0.880, while both AD and FTD patients showed higher synchronization than CN in faster bands, particularly Alpha (AD = 0.723, FTD = 0.720, CN = 0.660) and Beta (AD = 0.729, FTD = 0.713, CN = 0.681). This reversal suggests that healthy brains maintain coordinated slow-wave rhythms at rest, while disease groups exhibit abnormal hyper-synchrony at faster frequencies, reflecting a breakdown in the brain's ability to maintain functional independence between regions.

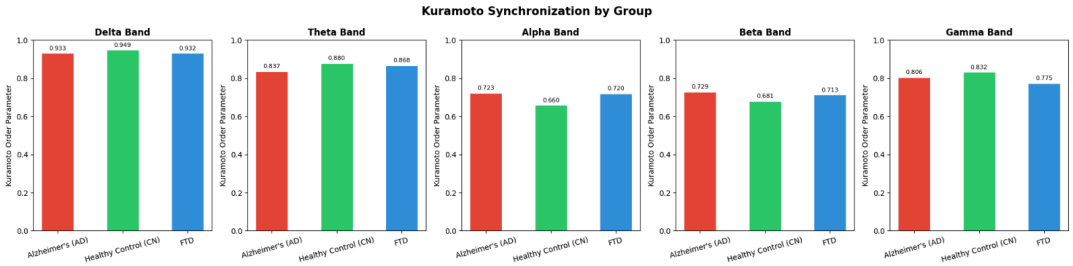

Figure 2: Kuramoto order parameter across five frequency bands — Delta, Theta, Alpha, Beta, and Gamma — for AD, CN, and FTD. Healthy Controls show higher synchronization in slower bands, while disease groups show elevated synchronization in faster bands.

Machine Learning Classification

Figure 3 shows the 5-fold cross-validation balanced accuracy for four machine learning models trained to classify subjects into AD, CN, and FTD groups using band power and Kuramoto synchronization features. All four models performed above the 33% chance level, confirming that the extracted EEG features carry meaningful diagnostic information. The tuned Support Vector Machine (SVM) achieved the highest balanced accuracy of 0.556, while the Neural Network showed the most consistent performance across folds with the tightest interquartile range. The Logistic Regression exhibited the highest variability, with one fold dropping below the chance level (0.23). The primary challenge across all models was distinguishing FTD from Healthy Controls, whose EEG signatures overlap considerably in feature space.

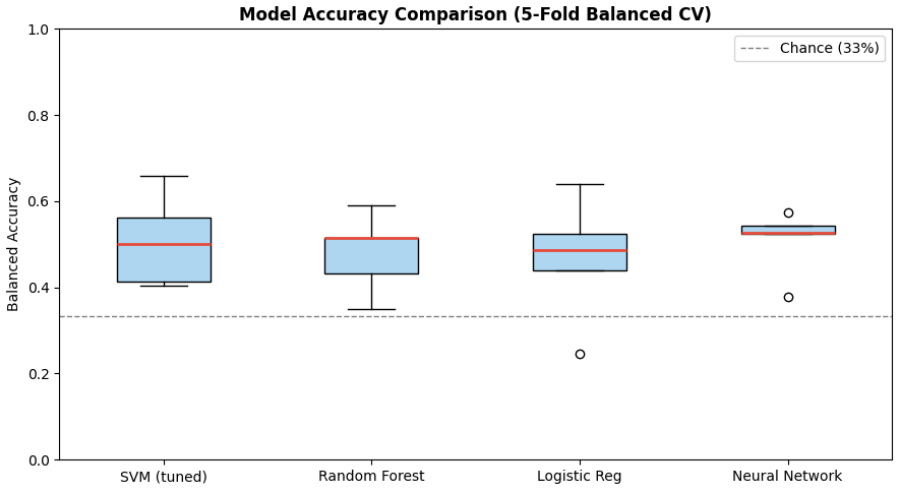

Figure 3: 5-fold cross-validation balanced accuracy for four machine learning models — SVM (tuned), Random Forest, Logistic Regression, and Neural Network. The dashed line indicates the 33% chance level. All models perform above chance, with SVM achieving the highest median accuracy of 0.556.

Electrode Importance

Figures 4a and 4b show the contribution of each electrode to group classification, computed using Random Forest feature importance across all five frequency bands. The five most important electrodes were O2 (0.0176), T5 (0.0149), O1 (0.0138), F7 (0.0119), and P3 (0.0116), spanning occipital, temporal, parietal, and frontal regions. In contrast, the midline electrodes Fp1, Fp2,

Fz, Cz, and Pz contributed negligibly, approaching zero importance. The topomap confirms this spatial pattern, with the largest and darkest green circles concentrated in posterior and left temporal regions, consistent with known patterns of neurodegeneration in AD and FTD.

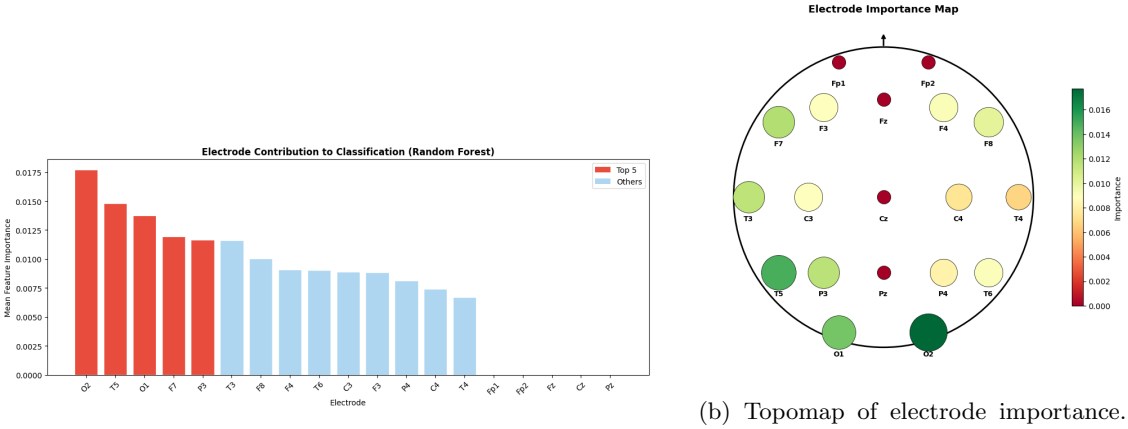

(a) Bar chart of mean feature importance per electrode. Top 5 electrodes highlighted in red.

(b) Topomap of electrode importance. Larger and greener circles indicate higher contribution.

Figure 4: Electrode contribution to group classification using Random Forest importance. Posterior and temporal electrodes O2, T5, and O1 show the highest importance, while midline electrodes Fp1, Fp2, Fz, Cz, and Pz contribute negligibly.

Electrode Coupling

Figure 5 shows the difference in Kuramoto electrode coupling between disease groups and Healthy Controls across all five frequency bands. In the Delta band, both AD and FTD showed predominantly weaker coupling than CN (blue), suggesting a loss of normal slow-wave connectivity. The most striking differences appeared in the Alpha and Beta bands, where both disease groups showed widespread stronger coupling than CN (red) across nearly all electrode pairs, consistent with the abnormal hyper-synchrony observed in the Kuramoto order parameter analysis. Figure 6 further reveals that Healthy Controls show the strongest Theta band coupling in frontal electrode pairs (FP2-F4, K = 0.945), while AD patients show a shift toward posterior pairs such as O2-T6 (K = 0.914), and FTD patients show almost exclusively posterior coupling dominated by occipital pairs such as P3-O1 (K = 0.921), reflecting a progressive disruption of long-range frontal neural communication associated with neurodegeneration.

Conclusion

This study presented a comprehensive EEG-based analysis framework for distinguishing between Alzheimer's Disease (AD), Frontotemporal Dementia (FTD), and Healthy Controls (CN) using a publicly available clinical dataset of 88 subjects from OpenNeuro. By combining band power analysis, Kuramoto synchronization, electrode coupling matrices, and machine learning classification, several consistent and neurologically meaningful patterns were identified.

AD patients exhibited elevated band power across all five frequency bands, consistent with known EEG biomarkers of diffuse cortical slowing, while FTD patients showed the lowest power across all bands, reflecting more focal neurodegeneration. Kuramoto analysis revealed a striking reversal — Healthy Controls showed greater synchronization in slower bands (Delta and Theta), while disease groups exhibited abnormal hyper-synchrony in faster bands (Alpha and Beta). Electrode coupling analysis identified a shift from frontal-dominated connectivity in healthy subjects

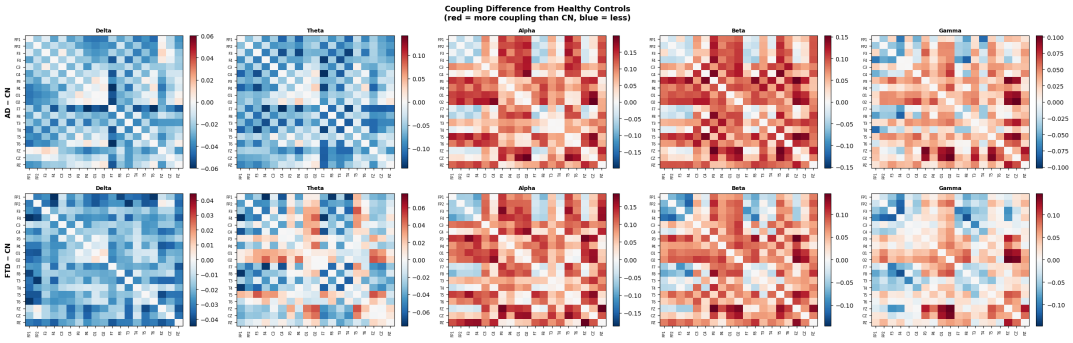

Figure 5: Coupling difference matrices between disease groups and Healthy Controls (CN) across five frequency bands. Red indicates stronger coupling than CN, blue indicates weaker coupling. Both AD and FTD show widespread hyper-connectivity in Alpha and Beta bands and reduced connectivity in Delta.

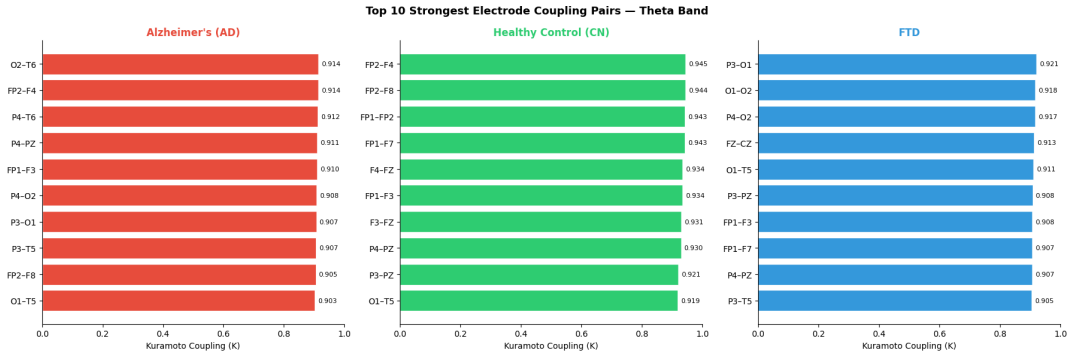

Figure 6: Top 10 strongest electrode coupling pairs in the Theta band for each group. Healthy Controls show frontal dominance (FP2-F4, FP1-FP2), while AD shows a mix of frontal and posterior pairs, and FTD shows almost exclusively posterior and occipital pairs, reflecting a progressive shift in dominant brain connectivity.

to posterior-dominated connectivity in disease groups, with widespread hyper-connectivity in Alpha and Beta bands confirmed across both AD and FTD. Random Forest importance analysis identified O2, T5, O1, F7, and P3 as the most diagnostically relevant electrodes, confirming that posterior and temporal regions carry the most discriminative EEG information.

Machine learning classification achieved a balanced accuracy of 55.6% using a tuned SVM, meaningfully above the 33% chance level, with FTD proving the most difficult group to classify due to its overlap with healthy controls in EEG feature space. Compared to existing studies, this work is unique in its simultaneous application of Kuramoto dynamics, full electrode coupling matrices, and three-way classification including FTD. Future work should explore larger datasets, additional EEG features, and integration with other neuroimaging modalities to improve classification accuracy and clinical applicability.

References

[1] Zaineb Ajra et al. "Using shallow neural networks with functional connectivity from EEG signals for early diagnosis of Alzheimer's and frontotemporal dementia". In: *Frontiers in Neurology* 14 (2023), p. 1270405. DOI: 10.3389/fneur.2023.1270405.

[2] Alzheimer's Association. "2026 Alzheimer's Disease Facts and Figures". In: *Alzheimer's Dementia* 22 (2026). DOI: 10.1002/alz.71345.

[3] Estela Area-Gomez and Eric A. Schon. "On the pathogenesis of Alzheimer's disease: the MAM hypothesis". In: *The FASEB Journal* 31.3 (2017), pp. 864–867. DOI: 10.1096/fj.201601309.

[4] Jee Bang, Salvatore Spina, and Bruce L. Miller. "Frontotemporal dementia". In: *The Lancet* 386.10004 (2015), pp. 1672–1682. DOI: 10.1016/S0140-6736(15)00461-4.

[5] Raymundo Cassani et al. "Systematic Review on Resting-State EEG for Alzheimer's Disease Diagnosis and Progression Assessment". In: *Disease Markers* 2018 (2018), p. 5174815. DOI: 10.1155/2018/5174815.

[6] David S Knopman et al. "Alzheimer disease". In: *Nature Reviews Disease Primers* 7.1 (2021), p. 33.

[7] Ira T Lott and Elizabeth Head. "Dementia in Down syndrome: unique insights for Alzheimer disease research". In: *Nature Reviews Neurology* 15.3 (2019), pp. 135–147.

[8] Andreas Miltiadous, Katerina D. Tzimourta, Theodora Afrantou, et al. "A Dataset of Scalp EEG Recordings of Alzheimer's Disease, Frontotemporal Dementia and Healthy Subjects from Routine EEG". In: *Data* 8.6 (2023), p. 95. DOI: 10.3390/data8060095.

[9] Andreas Miltiadous et al. *A dataset of EEG recordings from: Alzheimer's disease, Frontotemporal dementia and Healthy subjects*. OpenNeuro dataset ds004504. 2023. DOI: 10.18112/openneuro.ds004504.

[10] Sean M Nestor et al. "Ventricular enlargement as a possible measure of Alzheimer's disease progression". In: *Brain* 131.9 (2008), pp. 2443–2454.

[11] Katya Rascovsky et al. "Sensitivity of revised diagnostic criteria for the behavioural variant of frontotemporal dementia". In: *Brain* 134.9 (2011), pp. 2456–2477. DOI: 10.1093/brain/awr179.

[12] World Health Organization. *Dementia*. Fact sheet, updated March 31, 2025. 2025.